Electron Spin Resonance Studies of the Oxidation of $[Tc^{V}NCl_2(EPh_3)_2]$ (E = P or As) to $[Tc^{VI}NCl_4]^-$ by Thionyl Chloride: Structure of Dichloronitridobis(triphenylarsine)-technetium(V)†

John Baldas, John F. Boas, Silvano F. Colmanet and Geoffrey A. Williams
Australian Radiation Laboratory, Yallambie, Victoria 3085, Australia

The complexes $[Tc^{V}NCl_2(EPh_3)_2]$ (E = P or As) are oxidized to $[Tc^{VI}NCl_4]^-$ in thionyl chloride solution at room temperature. ESR spectroscopy has established the presence of technetium(VI) intermediates, $[TcNCl_3(EPh_3)]$: E = P, $g_{\|} = 2.0316$, $g_{\perp} = 2.0026$, $A_{\|} = 0.0267$ cm^{-1}, $A_{\perp} = 0.0119$ cm^{-1}, $Q = 0.000\,35$ cm^{-1}, $a_x = a_y = 0.0017$ cm^{-1}, $a_z = 0.00185$ cm^{-1}; E = As, $g_{\|} = 2.0246$, $g_{\perp} = 1.9986$, $A_{\|} = 0.0271$ cm^{-1}, $A_{\perp} = 0.0125$ cm^{-1}, $Q = 0.0003$ cm^{-1}, $a_x = a_y = 0.00195$ cm^{-1} and $a_z = 0.0021$ cm^{-1}. The crystal structure of $[TcNCl_2(AsPh_3)_2]$ **1** has been determined and is compared with those of $Re^{V}N$ and $Tc^{V}N$ phosphine complexes. Crystals of **1** are monoclinic, space group $I2/a$, with $a = 15.823(4)$, $b = 9.638(2)$, $c = 22.490(7)$ Å, $\beta = 101.91(2)°$ and $Z = 4$. Molecules of **1** possess C_2 symmetry with N≡Tc–Cl and N≡Tc–As angles of 110.51(3) and 99.22(1)°, respectively. The Tc≡N bond length is 1.601(5) Å.

The technetium(VI) nitrido complexes $R[TcNX_4]$ (R = $AsPh_4$ or NBu^n_4; X = Cl or Br) have been shown to be convenient starting materials for the preparation of a wide variety of $Tc^{V}N$ complexes by ligand substitution with concomitant reduction of Tc^{VI} to Tc^{V}.[1,2] Reduction has been found to occur even in substitution reactions by ligands such as pyridine and 2,2′-bipyridyl.[3,4] There are, however, examples other than halide-exchange reactions where the oxidation state Tc^{VI} is retained, such as the reaction of $[AsPh_4][TcNCl_4]$ with oxalic acid to give the cyclic tetramer $[AsPh_4]_4[Tc_4N_4O_2(ox)_6]$ [ox = oxalate(2−)][5] and of $[NBu^n_4][TcNCl_4]$ with *N*,*N*′-ethylene-bis(salicylideneimine) (H_2salen) to give [TcN(salen)]Cl.[6] Recently, we have reported the structure of the novel technetium(VI) dimer $[\{TcN(S_2CNEt_2)\}_2(\mu\text{-}O)_2]$, prepared by the reaction of $Na(S_2CNEt_2)$ with $[Tc_2N_2O_2(H_2O)_6]^{2+}$.[7] Previously, reaction of $Na(S_2CNEt_2)$ with $R[TcNCl_4]$ had resulted only in the isolation of $[Tc^{V}N(S_2CNEt_2)_2]$.[2]

The oxidation of $Tc^{V}N$ complexes by chlorine or bromine has been reported; ESR studies showed the presence of a number of intermediates with the final product being $[TcNX_4]^-$ (X = Cl or Br).[8,9] We are investigating the interconversion of $Tc^{VI}N^{3+}$ and $Tc^{V}N^{2+}$ cores and now report chemical and ESR studies of the oxidation of $[Tc^{V}NCl_2(EPh_3)_2]$ (E = P or As) to $[TcNCl_4]^-$ by thionyl chloride and subsequent reduction to $[TcCl_6]^{2-}$ under appropriate conditions. In order to establish the *trans* disposition of the chloro ligands and the magnitude of the N≡Tc–E and N≡Tc–Cl angles we have determined the X-ray structure of $[TcNCl_2(AsPh_3)_2]$ **1**.

Experimental

Thionyl chloride (analytical grade, containing less than 0.03% S_2Cl_2 + SCl_2) was obtained from Fluka, Switzerland. The $[TcNCl_2(EPh_3)_2]$ (E = P or As) complexes were prepared by the reaction of $[AsPh_4][TcNCl_4]$ with an excess of EPh_3 in MeCN.[2,10] Attempted preparation of the $SbPh_3$ analogue resulted in intractable products.

Reaction of $[TcNCl_2(AsPh_3)_2]$ **1** *with* $SOCl_2$.—A solution of complex **1** (40 mg, 0.050 mmol) in $SOCl_2$ (3 cm^3) was heated at reflux for 15 s. To the cooled orange-red solution was added $AsPh_4Cl$ (32 mg, 0.076 mmol) and the mixture taken to dryness on a rotary evaporator. Absolute ethanol was added to the residue and the orange-red crystals of $[AsPh_4][TcNCl_4]$ were collected by filtration and washed with ethanol. Yield 21 mg (66%). Recrystallisation from MeCN–benzene (1:1) gave crystals of m.p. 270–272 °C (lit.,[1] 272–274 °C). The IR spectrum was identical with that of $[AsPh_4][TcNCl_4]$ prepared by the literature method.[1]

Reaction of $[TcNCl_2(PPh_3)_2]$–$AsPh_4Cl$ *with* $SOCl_2$.—A solution of $[TcNCl_2(PPh_3)_2]$ (25 mg, 0.035 mmol) and $AsPh_4Cl$ (60 mg, 0.143 mmol) in $SOCl_2$ (4 cm^3) was heated under reflux for 35 min during which time the deep orange-red solution gradually became pale orange. The solution was evaporated to dryness on a rotary evaporator and the yellow residue extracted with refluxing absolute ethanol to remove excess of $AsPh_4Cl$ and PPh_3 reaction products. The residue was suspended in acetone to remove any $[AsPh_4][TcNCl_4]$ and the bright yellow crystals collected by filtration. Yield 23.6 mg {62% based on $[TcNCl_2(PPh_3)_2]$}. The m.p. and IR spectrum were identical with a sample of $[AsPh_4]_2[TcCl_6]$ prepared by the reduction of NH_4TcO_4 with HCl and precipitation with $AsPh_4Cl$.

Reaction of $[AsPh_4][TcNCl_4]$–PPh_3 *with* $SOCl_2$.—A mixture of $[AsPh_4][TcNCl_4]$ (20 mg, 0.031 mmol) and PPh_3 (33 mg, 0.126 mmol) dissolved in $SOCl_2$ (3 cm^3) was refluxed for 30 min. To the cooled pale orange-yellow solution was added $AsPh_4Cl$ (40 mg, 0.096 mmol) and the mixture treated as above to give $[AsPh_4]_2[TcCl_6]$ (26 mg, 77% yield).

X-Ray Crystallography.—Single crystals of $[TcNCl_2(AsPh_3)_2]$ **1** suitable for X-ray diffraction studies were grown by slow evaporation at room temperature of an acetonitrile solution. Accurate unit-cell parameters were determined at 22(1) °C by least-squares refinement of 2θ values measured with Cu-Kα radiation for 22 independent reflections well separated in reciprocal space.

Crystal data. $C_{36}H_{30}As_2Cl_2NTc$, $M = 796.30$, monoclinic, space group $I2/a$, $a = 15.823(4)$, $b = 9.638(2)$, $c = 22.490(7)$ Å,

† *Supplementary data available:* see Instructions for Authors, *J. Chem. Soc., Dalton Trans.*, 1991, Issue 1, pp. xviii–xxii.

Table 1 Atomic positional coordinates, with estimated standard deviations (e.s.d.s) in parentheses, for $[TcNCl_2(AsPh_3)_2]$

Atom	*X/a*	*Y/b*	*Z/c*
Tc	0.25	0.261 72(4)	0.0
As	0.366 99(2)	0.304 01(4)	0.094 32(2)
Cl	0.351 33(7)	0.348 0(1)	−0.055 31(5)
N	0.25	0.095 6(5)	0.0
C(1)	0.351 7(3)	0.208 3(4)	0.167 1(2)
C(2)	0.276 5(3)	0.132 8(4)	0.165 8(2)
C(3)	0.265 8(3)	0.058 5(5)	0.216 7(2)
C(4)	0.329 5(3)	0.061 6(6)	0.268 8(2)
C(5)	0.402 6(4)	0.136 9(7)	0.270 5(2)
C(6)	0.415 2(3)	0.210 2(6)	0.219 5(2)
C(7)	0.482 6(2)	0.245 5(4)	0.088 9(2)
C(8)	0.552 1(3)	0.334 2(5)	0.096 2(2)
C(9)	0.633 5(3)	0.283 2(5)	0.091 5(2)
C(10)	0.644 3(3)	0.145 6(5)	0.080 6(2)
C(11)	0.575 1(3)	0.056 8(5)	0.072 2(3)
C(12)	0.493 8(3)	0.107 4(5)	0.076 5(3)
C(13)	0.377 7(2)	0.499 3(4)	0.116 2(2)
C(14)	0.361 8(3)	0.545 8(5)	0.171 1(2)
C(15)	0.364 7(3)	0.688 4(5)	0.183 6(3)
C(16)	0.384 6(3)	0.780 6(5)	0.142 5(3)
C(17)	0.400 7(5)	0.734 4(5)	0.088 7(3)
C(18)	0.397 5(4)	0.593 2(5)	0.074 1(2)

$\beta = 101.91(2)°$, $U = 3355.9$ Å^3, $Z = 4$, $D_c = 1.58$ g cm^{-3}, μ(Cu-Kα) = 69.97 cm^{-1}.

Integrated intensities were measured on a Siemens AED diffractometer with nickel-filtered Cu-Kα radiation. A total of 3243 unique reflections were measured to a maximum (sinθ)/λ = 0.63 Å^{-1}, and the 2621 for which $I_o > 2\sigma(I_o)$ were used for the structure analysis. Three reflections, monitored every 50, showed no significant variation in intensities. The intensities were corrected for Lorentz and polarization effects, and for absorption (transmission factors ranged from 0.3405 to 0.6034).[11]

Structure refinement. The sites of the Tc, As, N and Cl atoms were taken from the isostructural $[ReNCl_2(PPh_3)_2]$.[12] Subsequent difference syntheses using SHELX 76[13] revealed the sites of all the remaining non-hydrogen atoms. The hydrogen atoms of the phenyl rings were included in the analysis at calculated positions (C–H = 1.08 Å) and assigned a variable overall isotropic thermal parameter. Full-matrix least-squares refinement, with anisotropic thermal parameters given to the non-hydrogen atoms, converged with $R = \Sigma\Delta F/\Sigma|F_o| = 0.032$, $R' = [\Sigma w(\Delta F)^2/\Sigma w|F_o|^2]^{\frac{1}{2}} = 0.038$, with $\chi = 1.26$ {defined as $[\Sigma w(\Delta F)^2/(N_o - N_v)]^{\frac{1}{2}}$} for 2621 data ($N_o$) and 193 variables ($N_v$). The function minimized was $\Sigma w(\Delta F)^2$ (where $\Delta F = ||F_o| - |F_c||$), with the data weighted according to $w = (\sigma^2|F_o| + 4 \times 10^{-4}|F_o|^2)^{-1}$. The largest peaks on the final difference map were of heights +0.55 and −0.32 e Å^{-3}. An isotropic extinction parameter of the form $F_c = F[1 - (1.28 \times 10^{-7}|F^2|/\sin\theta)]$ was applied to the calculated structure amplitudes.

Neutral-atom scattering-factor curves were taken from refs. 14, 15 and 16 for the non-hydrogen and hydrogen atoms, respectively. Anomalous dispersion corrections were applied to the non-hydrogen atoms.[11] Final atomic positional coordinates are given in Table 1. Fig. 3 was prepared from the output of ORTEP.[17]

Additional material available from the Cambridge Crystallographic Data Centre comprises H-atom coordinates, thermal parameters and remaining bond lengths and angles.

ESR Spectroscopy.—The ESR spectra were recorded with the use of a Bruker ESR-200D-SRC spectrometer and associated equipment. All solutions were 2 × 10^{-3} mol dm^{-3} in Tc.

(*a*) $[AsPh_4][TcNCl_4]$ *in* $SOCl_2$ *solution.* The spectrum of a solution of $[AsPh_4][TcNCl_4]$ in $SOCl_2$ at room temperature and after freezing to 130 K exhibited similar features to those observed for $[TcNCl_4]^-$ in other non-aqueous solvents.[18] The signal intensity corresponded to all of the Tc present and remained unchanged on standing. At room temperature the 10-line spectrum due to ^{99}Tc ($I = \frac{9}{2}$) was observed and there was no evidence of resolved superhyperfine structure due to chlorine.

In solutions frozen to 130 K the 'parallel' peaks at both low and high fields exhibited a field-dependent splitting characteristic of the presence of two species with slightly different values of $g_{||}$ and $A_{||}$. Addition of 0.5 mol dm^{-3} $AsPh_4Cl$ to the solution prior to freezing resulted in the disappearance of one of the species. Since this solution contains a large excess of chloride ion the remaining spectrum is identified as being due to $[TcNCl_5]^{2-}$. The other species is therefore $[TcNCl_4]^-$ with the sixth position (*trans* to nitrogen) either vacant or, more likely, occupied by a weakly co-ordinated $SOCl_2$ molecule. The above observations represent the first evidence of an equilibrium between $[TcNCl_4]^-$ and $[TcNCl_5]^{2-}$ in solution, although similar equilibria between $[TcOCl_4]^-$ and $[TcOCl_5]^{2-}$ and $[MoOCl_4]^-$ and $[MoOCl_5]^{2-}$ are well established.[19,20] It may be noted that the chloro ligands of $[TcNCl_4]^-$ most likely undergo exchange with $SOCl_2$. This is indicated by the rapid conversion of deep blue $[AsPh_4][TcNBr_4]$ *into orange* $[AsPh_4][TcNCl_4]$ on dissolution in $SOCl_2$.

(*b*) $[TcNCl_2(PPh_3)_2]$ *and* $[TcNCl_2(AsPh_3)_2]$ *in* $SOCl_2$ *solution.* Polycrystalline powders of both these technetium(v) complexes exhibited no ESR spectra at room temperature and at 130 K. On addition of $SOCl_2$ a green colour developed which gradually turned yellow-brown. For solutions of $[TcNCl_2(PPh_3)_2]$ these changes occurred over a period of between 10 and 20 min, whilst for solutions of $[TcNCl_2(AsPh_3)_2]$ the green colour only persisted for about 90 s.

The spectrum of $[TcNCl_2(PPh_3)_2]$ in $SOCl_2$ at room temperature, when examined during the first few minutes after dissolution, exhibited the 10-line spectrum characteristic of a technetium(VI) complex tumbling in solution. The increase in intensity of this signal paralleled the development of the green colour. The width of each component line was between 4.0 and 5.2 mT, but no evidence for chlorine or phosphorus superhyperfine coupling could be observed. After 10 min a second 10-line spectrum with linewidths between 1.5 and 2.0 mT appeared and gradually increased in intensity. This spectrum was identical to that observed from the solutions of $[AsPh_4][TcNCl_4]$ in $SOCl_2$.

Similar observations were made from $SOCl_2$ solutions of $[TcNCl_2(AsPh_3)_2]$ when examined at room temperature, although here the lines of the initial 10-line spectrum were rather broader, *ca.* 12 mT. The initial spectrum faded rapidly and was not observed after about 2 min. The only spectrum observed at longer times was that exhibited by solutions of $[AsPh_4][TcNCl_4]$ in $SOCl_2$. The best solution spectrum of $[TcNCl_2(AsPh_3)_2]$ in $SOCl_2$ was obtained when the temperature of the nitrogen gas flowing through the cavity Dewar insert was reduced to *ca.* 240 K. This slowed the reaction sufficiently to enable the spectrum of the intermediate species to be observed without interference from resonances due to $[TcNCl_4]^-$ or $[TcNCl_5]^{2-}$. No superhyperfine structure due to Cl or As was observed.

The nature of the intermediate species is clarified by the ESR spectra of solutions frozen to 130 K. These solutions, when frozen shortly after addition of $SOCl_2$ to $[TcNCl_2(AsPh_3)_2]$ or $[TcNCl_2(PPh_3)_2]$, exhibited spectra largely due to a single species in each case. As shown in Figs. 1 and 2, the parallel features show splittings due to the interaction of the technetium ion with a single P ($I = \frac{1}{2}$) or As ($I = \frac{3}{2}$) nucleus, respectively. The perpendicular features, although broader than those of $[TcNCl_5]^{2-}$, exhibited no resolved superhyperfine structure.

The ESR spectra of solutions frozen at longer times after addition of $SOCl_2$ (greater than *ca.* 10 min for P, and *ca.* 60 s for

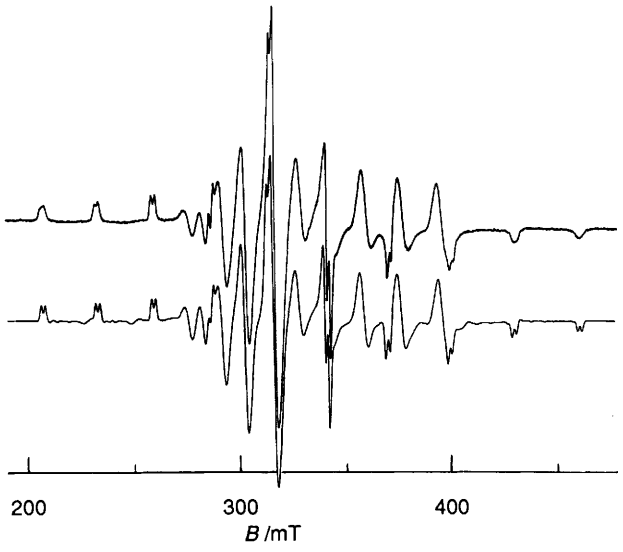

Fig. 1 The ESR spectrum of $[TcNCl_2(PPh_3)_2]$ in $SOCl_2$ (2×10^{-3} mol dm^{-3}) when frozen to 130 K 5 min after addition of solvent (upper curve). The lower curve is the spectrum simulated by use of the parameters in Tables 2 and 3. The linewidths used in the simulations were $\sigma_{\parallel} = 0.6$ mT and $\sigma_{\perp} = 1.60$ mT, but strain-broadening effects were not taken into account. Spectrometer conditions: microwave frequency 9.522 GHz, microwave power 20 mW, spectrometer gain 2.5×10^4, 100 kHz modulation amplitude 0.4 mT

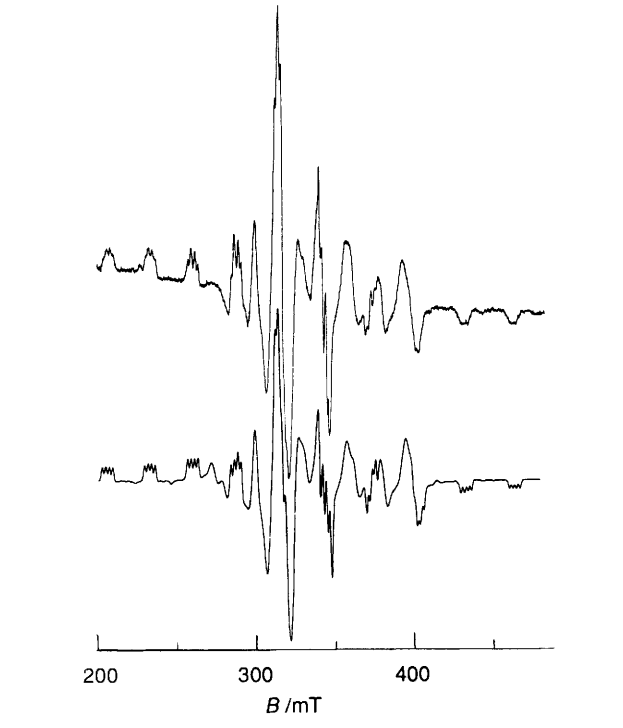

Fig. 2 The ESR spectrum of $[TcNCl_2(AsPh_3)_2]$ in $SOCl_2$ (2×10^{-3} mol dm^{-3}) when frozen to 130 K approximately 30 s after addition of solvent (upper curve). The lower curve is the spectrum simulated by use of the parameters in Tables 2 and 3. The linewidths used in the simulations were $\sigma_{\parallel} = 0.8$ mT and $\sigma_{\perp} = 1.60$ mT, but strain-broadening effects were not taken into account. Parts of the experimental spectrum are distorted because of the presence of small amounts of $[TcNCl_4]^-$ and its adducts. Spectrometer conditions: microwave frequency 9.524 GHz, microwave power 20 mW, spectrometer gain 10×10^4, 100 kHz modulation amplitude 0.5 mT

As) showed clear evidence for the presence of $[TcNCl_4]^-$ and its adducts. Their intensity increased with time, whilst the intensity of the intermediate species which exhibited phosphorus or arsenic superhyperfine structure gradually decreased. After longer times (5 h for P, and 10 min for As) only $[TcNCl_4]^-$ and its adducts were observed. The intensity corresponded to *ca.* 50% of the Tc present in solution. Solutions left for several days prior to freezing exhibited less-intense signals due to $[TcNCl_4]^-$ and its adducts but a broad resonance, peak-to-peak width *ca.* 20 mT and centred around $g = 2$, was observed. This broad resonance is probably due to solute aggregation.

Spin Hamiltonian Parameters and Spectral Simulations.—The spectra of $[TcNCl_4]^-$, $[TcNCl_5]^{2-}$ and of the PPh_3 and $AsPh_3$ intermediates were simulated as described previously.[21] The standard spin Hamiltonian (1) was used where $S = \frac{1}{2}$, $I = \frac{9}{2}$

$$\mathcal{H} = g_{\parallel}\beta B_z S_z + g_{\perp}\beta(B_x S_x + B_y S_y) + A_{\parallel} S_z I_z + A_{\perp}(S_x I_x + S_y I_y) + Q[I^2{}_z - I(I+1)/3] + \mathcal{H}_{s.h.f.} \quad (1)$$

(for Tc), $\mathcal{H}_{s.h.f.}$ is the ligand superhyperfine term and the other terms have their usual meanings. For the systems discussed here, both the g matrix and the A tensor were found to be axially symmetric.

For $[TcNCl_4]^-$ and $[TcNCl_5]^{2-}$ the chlorine superhyperfine (s.h.f.) interaction was treated as described previously.[21] Although no chlorine s.h.f. splitting was observed for either room-temperature solutions or solutions frozen to 130 K, the isotropic chlorine s.h.f. interaction could be estimated from the linewidths of the room-temperature spectrum. Given the appropriate combination of signs for the anisotropic components, the isotropic constant, $a_0 = 0.5 \times 10^{-4}$ cm^{-1}, is consistent with the s.h.f. components estimated from the frozen-solution spectra. These are in good agreement with the values obtained from single-crystal and electron nuclear double resonance (ENDOR) studies.[22] The spin Hamiltonian parameters are given in Tables 2 and 3.

For the PPh_3 and $AsPh_3$ intermediates only the component of the superhyperfine interaction parallel to the symmetry axis, a_z, could be determined directly. The isotropic superhyperfine interaction constant, a_0, was estimated from simulations of solution-phase spectra which included different trial values of a_0 and linewidth (Table 3).

The phosphorus and arsenic s.h.f. interaction constants perpendicular to the ESR symmetry axis were estimated from a_z and a_0. The best fits were obtained with the values given in Table 3. It was necessary to include an anisotropic component in the linewidth to achieve a satisfactory agreement between experimental and computed spectra. This is assumed to arise from the unresolved chlorine s.h.f. interaction. Suitable widths are obtained when three chlorine nuclei are included in the calculations, each with a s.h.f. interaction similar to that found for the equatorial chlorines in $[TcNCl_5]^{2-}$.

Results and Discussion

We have recently reported that $[AsPh_4][TcOCl_4]$ is only slowly reduced by reflux in $SOCl_2$, but that in the presence of added $AsPh_4Cl$ reduction occurs rapidly to give $[AsPh_4]_2[TcCl_6]$, which may be isolated in high yield.[24] The TcN^{n+} ($n = 2$ or 3) cores have been shown to have a much greater stability than the TcO^{3+} core,[1,2] but $[AsPh_4]_2[TcN(mnt)_2]$ [mnt = 1,2-dicyanoethenedithiolate(2−)-*S*,*S*′] has been reported to be converted into $[AsPh_4]_2[TcCl_6]$ by reflux in $SOCl_2$.[25] The $[AsPh_4][TcNCl_4]$ complex was unaffected by reflux in $SOCl_2$ for 1 h. Reflux in the presence of added $AsPh_4Cl$ (1 equivalent) resulted in the formation of only traces of $[AsPh_4]_2[TcCl_6]$.

A solution of $[TcNCl_2(AsPh_3)_2]$ in $SOCl_2$ was converted into orange $[TcNCl_4]^-$ over several minutes on standing at room temperature. The rate of conversion was accelerated by heating and a 66% yield of $[AsPh_4][TcNCl_4]$ was obtained on addition of $AsPh_4Cl$. In the case of $[TcNCl_2(PPh_3)_2]$ the conversion into $[TcNCl_4]^-$ at room temperature occurred over a period of hours. From the briefly heated reaction mixture only

Table 2 Spectral parameters. All hyperfine and quadrupole interaction parameters are given in units of $\times 10^4$ cm^{-1}; g_0 and A_0 were obtained from the spectra of the liquid phase

System	T/K	$g_{\|}$ ($\pm$0.0005)	$g_{\perp}$ ($\pm$0.0005)	$A_{\|}$ ($\pm$0.2)	$A_{\perp}$ ($\pm$0.2)	Q ($\pm$0.5)	β_2^2
[AsPh$_4$][TcNCl$_4$] in SOCl$_2$ + 0.5 mol dm^{-3} AsPh$_4$Cl	300	g_0 = 2.006 ($\pm$0.002)		A_0 = 186.0 ($\pm$2.0)			
	130	2.0076	2.0025	292.0	131.0	5.2	0.77
[TcNCl$_3$(PPh$_3$)] in SOCl$_2$	300	g_0 = 2.015 ($\pm$0.003)		A_0 = 170.0 ($\pm$2.0)			
	130	2.0316	2.0026	267.0	119.0	3.5	0.74
[TcNCl$_3$(AsPh$_3$)] in SOCl$_2$	250	g_0 = 2.015 ($\pm$0.003)		A_0 = 170.0 ($\pm$4.0)			
	130	2.0246	1.9986	271.0	125.0	3.0	0.72
[Tc^{II}(NS)Cl$_3$(PMe$_2$Ph)$_2$][23]	130	2.027	2.039	236.7	106.3	—	0.77

Table 3 ESR spectral parameters (ligand superhyperfine interactions) in SOCl$_2$ solution. All superhyperfine interactions are given in units of $\times 10^4$ cm^{-1}; a_0 was obtained from the spectra of the liquid phase

System	a_0	a_x	a_y	a_z	f_s(%)	f_p(%)
[AsPh$_4$][TcNCl$_4$] + 0.5 mol dm^{-3} AsPh$_4$Cl	<0.5 ($\pm$1.0)	3.0 ($\pm$1.0)	6.0 ($\pm$1.0)	0.5	<0.04	5.2
[TcNCl$_3$(PPh$_3$)]	18.0 ($\pm$2.0)	17.0 ($\pm$1.0)	17.0 ($\pm$1.0)	18.5 ($\pm$0.5)	0.52	0.61
[TcNCl$_3$(AsPh$_3$)]	23.0 ($\pm$3.0)	19.5 ($\pm$1.0)	19.5 ($\pm$1.0)	21.0 ($\pm$0.5)	0.64	0.56

a low yield of [AsPh$_4$][TcNCl$_4$] was obtained. This was due to the reduction of [TcNCl$_4$]$^-$ to [Tc^{IV}Cl$_6$]$^{2-}$ which was obtained in 49% yield as [AsPh$_4$]$_2$[TcCl$_6$].

These results show that the Tc^{V}N complexes are first oxidized to [Tc^{VI}NCl$_4$]$^-$ by SOCl$_2$ and that the [TcNCl$_4$]$^-$ is then reduced to [Tc^{IV}Cl$_6$]$^{2-}$. The relative ease of the oxidation and reduction steps depends on the ligands present. Thus, the oxidation of [TcNCl$_2$(AsPh$_3$)$_2$] is more rapid than that of [TcNCl$_2$(PPh$_3$)$_2$] but the subsequent reduction of [TcNCl$_4$]$^-$ occurs more readily in the latter case. The reduction of [TcNCl$_4$]$^-$ to [TcCl$_6$]$^{2-}$ in SOCl$_2$ apparently requires the presence of a reducing ligand. This was demonstrated by the observation that [AsPh$_4$][TcNCl$_4$] was unaffected by reflux in SOCl$_2$ but was readily reduced to [TcCl$_6$]$^{2-}$ on addition of PPh$_3$.

ESR Spectroscopy.—When [TcNCl$_2$(PPh$_3$)$_2$] or [TcNCl$_2$(AsPh$_3$)$_2$] was dissolved in SOCl$_2$ a single ESR-detectable intermediate was observed in each case. The spectra of these species showed evidence for the co-ordination of only one P- or As-containing ligand to Tc. The almost isotropic s.h.f. interaction for P and As contrasts with the quite anisotropic interaction observed for halogeno ligands in species such as [TcNCl$_4$]$^-$.

The g and A values for the P- and As-co-ordinated intermediate species are consistent with the unpaired electron being substantially in an orbital of b_2 symmetry, *i.e.* $4d_{xy}$. The reduction of Tc^{V}N complexes by S_2Cl_2 has resulted in the formation of either technetium-(III), -(II) ($4d^5$-low spin) or -(I) thionitrosyl complexes.[26,27] In the present case, reduction to Tc^{II} would result in the formation of [Tc(NS)Cl$_3$(EPh$_3$)$_2$] (E = P or As). However, the g and A values, particularly $A_{\|}$, for technetium(II) thionitrosyl complexes are quite different to those of technetium(VI) nitrido complexes.[23] The g and A values observed here unequivocally show that the intermediate is a Tc^{VI}N species. Furthermore, they are similar to those found for species such as [TcNCl$_3$Br]$^-$ (ref. 28) and [TcNCl$_3$(CN)]$^-$,[29] suggesting that the intermediate species only differs from [TcNCl$_4$]$^-$ by one equatorial or near-equatorial ligand. Whilst it may be expected that the ESR spectrum of the intermediate species should exhibit rhombic or monoclinic symmetry (*cf.* some MoOCl$_3$L complexes),[30,31] no low-symmetry effects were observed. It should be noted that the ESR spectra of mixed-ligand species such as [TcNCl$_3$X]$^-$ (X = F, Br or CN) also do not show lower than axial symmetry.[21,28,29]

The most likely structure of the ESR-detectable intermediate is [TcNCl$_3$(EPh$_3$)], resulting from substitution of one of the EPh$_3$ ligands by chloride and oxidation to Tc^{VI} or by substitution by 'Cl' with concomitant oxidation. Structures in which a second EPh$_3$ ligand is strongly bound appear to be excluded by the absence of additional s.h.f. structure or line broadening. A structure of the form [TcNCl$_4$(EPh$_3$)]$^-$, with the EPh$_3$ ligand *trans* to the nitrogen, also seems unlikely in view of the observation that the ESR spectrum at 130 K of a frozen solution of [AsPh$_4$][TcNCl$_4$] in CH$_2$Cl$_2$ (a weakly co-ordinating solvent) to which PPh$_3$ (which is more reactive than AsPh$_3$) had been added (1:1) showed no evidence of PPh$_3$ co-ordination. Similarly, no changes were observed in a frozen solution of [AsPh$_4$][TcNCl$_4$] to which a large excess of OPPh$_3$ had been added. The strong *trans* influence of the nitrido ligand may well prevent the formation of octahedral adducts of the type *trans*-[TcNCl$_4$(EPh$_3$)]$^-$, although a rhenium analogue [AsPh$_4$][ReNCl$_4$(PPh$_3$)] has been isolated.[32]

An analysis of the various readily accessible bonding parameters with the aid of the expressions given in the Appendix shows that the bonding of the EPh$_3$ ligand is different to that of the equatorial chloro ligands in [TcNCl$_5$]$^{2-}$. It can be seen that the complexes involving co-ordination to PPh$_3$ or AsPh$_3$ are rather more covalent than [TcNCl$_5$]$^{2-}$, as shown by the smaller value of β_2^2 in Table 2. Furthermore, the electron density in the P and As s orbitals (as calculated from the isotropic s.h.f. interaction) is much larger, and that in the P and As p orbitals (as calculated from the anisotropic s.h.f. interaction) rather smaller than for the equatorial chloro ligands in [TcNCl$_5$]$^{2-}$. Whilst the s.h.f. interaction due to the chloro ligands in the [TcNCl$_3$(EPh$_3$)] intermediates could only be estimated from the linewidths, it appears to be similar to that for [TcNCl$_4$]$^-$ or [TcNCl$_5$]$^{2-}$, *i.e.* quite anisotropic.

The anisotropic chlorine s.h.f. coupling in [TcNCl$_4$]$^-$ and similar Tc^{VI}N complexes is ascribed to the fact that in C_{4v} symmetry the only ligand orbitals able to overlap with the $4d_{xy}$ ground state are the π orbitals in the basal plane directed perpendicular to the metal–ligand bond. This argument is analogous to that used for a number of molybdenum and niobium oxohalogeno complexes.[33]

The almost isotropic P and As s.h.f. coupling requires explanation. The magnitude of the s.h.f. interactions are similar to those observed for some phosphine and arsine adducts of VCl$_4$,

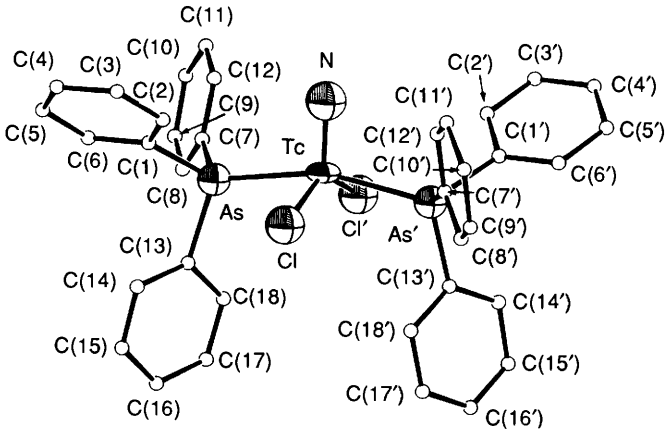

Fig. 3 A perspective view of $[TcNCl_2(AsPh_3)_2]$ **1** including the atom numbering scheme. Thermal ellipsoids are drawn at the 30% probability level. Primed atoms are related to the corresponding unprimed atoms by the two-fold axis

Table 4 Selected interatomic distances (Å) and angles (°) for $[TcNCl_2(AsPh_3)_2]$ **1**

Tc–N	1.601(5)	Tc–Cl	2.373(1)
Tc–As	2.5440(4)	As–C(1)	1.937(4)
As–C(7)	1.941(4)	As–C(13)	1.944(4)
N–Tc–Cl	110.51(3)	N–Tc–As	99.22(1)
As–Tc–Cl	85.81(3)	C(1)–As–Tc	115.6(1)
C(1)–As–C(7)	101.5(2)	C(1)–As–C(13)	105.5(2)
C(7)–As–Tc	115.7(1)	C(7)–As–C(13)	105.3(2)
C(13)–As–Tc	112.1(1)		

$NbCl_4$ and $TaCl_4$, where the symmetry is assumed to be C_{4v} and for which spin polarization has been suggested as the cause of the isotropic s.h.f. interaction.[34–36] However, as discussed above, the symmetry of the phosphine and arsine complexes reported here is likely to be lower than C_{4v}. This allows the possibility that the ground-state orbital is predominantly $|x^2 - y^2\rangle$, rather than $|xy\rangle$ as is assumed for $[TcNCl_4]^-$.[21] The ESR spectra are consistent with either ground state. As discussed by Hitchman *et al.*,[37] the ground state in the expected low-symmetry situation may be written as $\psi_1 = a|x^2 - y^2\rangle + b|xy\rangle + c|3z^2 - r^2\rangle$ where $a \gg b, c$. The presence of $|x^2 - y^2\rangle$ allows the admixture of s-orbital character from the equatorial ligands *via* sp hybridization, and hence would give rise to the observed s.h.f. interaction.

It should be noted that the nitrogen s.h.f. interaction in vanadyl porphyrin, which has C_{4v} symmetry, has been explained as arising from configurational mixing of $|x^2 - y^2\rangle$ character into the $|xy\rangle$ ground state.[38] Thus, polarization of the s-electron density at the P or As nucleus by unpaired spin in the ligand p orbitals or by unpaired spin in the metal d orbitals may not be required and would appear to lead to a rather more anisotropic s.h.f. interaction than is observed. These considerations lead to the conclusion that although the bonding to the EPh_3 ligand in the intermediate species is different to that of the chloro ligands, the overall structure is similar to that of the $[TcNCl_2(EPh_3)_2]$ precursor.

Molecular Structure of $[TcNCl_2(AsPh_3)_2]$ **1**.—The crystal structure consists of discrete $[TcNCl_2(AsPh_3)_2]$ molecules. A perspective view, which includes the atom numbering, is shown in Fig. 3, and selected interatomic distances and angles are given in Table 4.

The technetium(V) atom is co-ordinated to one nitrogen, two chlorine and two $AsPh_3$ ligands to give a distorted square pyramid with the nitrogen in the apical position. The technetium and nitrogen atoms lie on a crystallographically imposed two-fold axis, and thus the complex has exact C_2 symmetry. Although the basal ligands are severely distorted from planarity, as shown by the disparity between the N≡Tc–Cl angle of 110.51(3)° and the N≡Tc–As angle of 99.22(1)°, the angles are similar to those observed in other five-co-ordinate technetium nitrido complexes.[39] The Tc≡N bond length of 1.601(5) Å is similar to those observed in other five-co-ordinate technetium nitrido complexes[39] and the Tc–Cl bond length of 2.373(1) Å is unexceptional.[40] The bond lengths and angles in the co-ordination spheres of **1** and $[ReNCl_2(PPh_3)_2]$ are, except for the Tc–As and Re–P distances, closely similar (Table 5). The Tc–As bond length of 2.544(1) Å in **1** is comparable to those reported for the six-co-ordinate *trans*-$[Tc(pdma)_2Cl_2]A$ [pdma = *o*-phenylenebis(dimethylarsine)] [mean Tc–As: 2.515(2), A = ClO_4; 2.508(1) Å, A = Cl][44] and the eight-co-ordinate $[Tc(pdma)_2Cl_4]PF_6$ [2.578(2) Å].[45]

The influence of steric factors on Re≡N bond lengths has been studied with respect to the origin of the *trans* influence[12,43] (Table 5). The Re≡N bond length of 1.602(9) Å in five-co-ordinate $[ReNCl_2(PPh_3)_2]$[12] increases to 1.660(8) and 1.788(11) Å in six-co-ordinate $[ReNCl_2(PMe_2Ph)_3]$[42] and $[ReNCl_2(PEt_2Ph)_3]$,[43] respectively. The Tc≡N bond lengths of 1.601(5) Å for **1** and 1.624(4) Å for $[TcNCl_2(PMe_2Ph)_3]$[41] parallel the trend observed for the rhenium analogues. However, the Re≡N bond length in $[ReNCl_2(PMe_2Ph)_3]$ is significantly longer than the Tc≡N bond length in $[TcNCl_2(PMe_2Ph)_3]$ (Table 5). The *trans* influence of the nitrido ligand in $[TcNCl_2(PMe_2Ph)_3]$ is apparent in the *cis* and *trans* Tc–Cl bond lengths of 2.441(1) and 2.665(1) Å, respectively.[41]

A crystal structure of $[TcNCl_2(PEt_2Ph)_3]$ is not available, but the six-co-ordinate *trans*-$[TcN(Cl)(dmpe)_2]BPh_4$ [dmpe = 1,2-(dimethylphosphino)ethane], where there are four phosphorus donor atoms in the co-ordination sphere, has been reported to show the exceptionally long Tc≡N distance of 1.854(6) Å.[46] This distance seems to us to be unreasonably long, and it is possible that some small disorder between the *trans* nitrido and chloro ligands in the structure of $[TcN(Cl)(dmpe)_2]^+$ is responsible.

Conclusion

The oxidation of $[TcNCl_2(EPh_3)_2]$ (E = P or As) to $[TcNCl_4]^-$ by $SOCl_2$ occurs *via* the technetium(VI) intermediate $[TcNCl_3(EPh_3)]$. The geometry of this intermediate has been shown by ESR spectroscopy to most likely be distorted square pyramidal with the nitrido ligand in the apical position.

Appendix

For d^1 complexes with C_{4v} symmetry the molecular orbital of the unpaired electron may be written as in equation (A1) where

$$\varphi(B_2) = \beta_2|d_{xy}\rangle - \beta_2'|\varphi_1\rangle \quad \text{(A1)}$$

φ_1 represents the linear combination of the ligand orbitals. Following the approach of McGarvey,[47] we estimate the fraction of the unpaired electron density on the Tc atom, from equations (A2) and (A3), where $K = \kappa\beta_2^2P$ (κ is the Fermi

$$A_{\parallel} = -K - \tfrac{4}{7}\beta_2^2P + (g_{\parallel} - g_e)P + \tfrac{3}{7}(g_{\perp} - g_e)P \quad \text{(A2)}$$

$$A_{\perp} = -K + \tfrac{2}{7}\beta_2^2P + \tfrac{11}{14}(g_{\perp} - g_e)P \quad \text{(A3)}$$

isotropic contact interaction constant), g_e is the free-electron g factor, $P = g_e g_n \beta_e \beta_n \langle r^{-3}\rangle$ where g_n is the nuclear g factor, β_e and β_n are the Bohr and nuclear magnetons, respectively, and $\langle r^{-3}\rangle$ is the expectation value of the $4d_{xy}$ electron density for the technetium ion. Following the arguments of Manoharan and Rogers[48] and of McGarvey[47] for the isoelectronic molybdenum(V) ion, we estimate $P = 0.0245\ cm^{-1}$. Since both $A_{\parallel}$ and

Table 5 Selected interatomic distances (Å) and angles (°) for technetium and rhenium complexes $[MNCl_2(ER_3)_n]$ (E = P or As, n = 2 or 3)

Complex	M≡N	M–Cl	M–E	N≡M–Cl	N≡M–E	Ref.
$[TcNCl_2(AsPh_3)_2]$	1.601(5)	2.373(1)	2.544(1)	110.51(3)	99.22(1)	*a*
$[TcNCl_2(PMe_2Ph)_3]$	1.624(4)	2.441(1)	2.444(1)	104.7(2)	93.5(2)	41
		2.665(1)[b]	2.487(1)	170.5(2)	91.3(2)	
			2.486(1)		92.0(2)	
$[ReNCl_2(PPh_3)_2]$	1.602(9)	2.377(2)	2.448(2)	109.69(6)	98.44(5)	12
$[ReNCl_2(PMe_2Ph)_3]$	1.660(8)	2.442(2)	2.467(2)	103.8(3)	91.4(3)	42
		2.633(2)[b]	2.421(2)	172.2(3)	94.5(3)	
			2.469(2)		91.0(3)	
$[ReNCl_2(PEt_2Ph)_3]$	1.788(11)	2.454(4)	2.490(5)	99.2(4)	91.8(4)	43
		2.563(4)[b]	2.442(4)	176.4(4)	95.6(4)	
			2.469(5)		89.1(4)	

All the six-co-ordinate complexes are the *cis-mer* isomers. [a] This work. [b] Ligand *trans* to nitrido.

$A_\perp$ are negative, the values of β_2^2 listed in Table 2 can be calculated. Whilst the actual symmetry of the $[TcNCl_3(EPh_3)]$ (E = P or As) intermediates must be lower than C_{4v}, this is not shown by the ESR spectra, so that the expressions used above are at least a useful approximation.

It is convenient to write expressions for the components of the ^{31}P or ^{75}As superhyperfine tensors in the forms[49] (A4) and (A5)

$$a_{\|} = a_0 + 2a_d + 2(a_\sigma - a_\pi) \quad \text{(A4)}$$

$$a_\perp = a_0 - a_d - (a_\sigma - a_\pi) \quad \text{(A5)}$$

where $a_{\|}$ and $a_\perp$ refer to the superhyperfine components parallel and perpendicular to the Tc–P(As) bond axis, a_0 is the isotropic component, a_d represents the contribution from the dipole–dipole interaction of the electronic magnetic moment of the central ion and the magnetic moment of the ligand nucleus and a_σ and a_π represent the interactions through the ligand σ and π orbitals, respectively.

For the following analysis we assume that the Tc–E (E = P or As) bond is perpendicular to the Tc≡N direction, *i.e.* perpendicular to the parallel or z-axis direction used in the analysis of the technetium hyperfine structure. In the axis system we have used previously[18,21] this means that $a_{\|} = a_x$ and $a_\perp = a_z$. The only component determined directly from the ESR spectra is a_z, as the additional linewidth introduced by the chlorine superhyperfine interactions makes the direct determination of both a_x and a_y a task for ENDOR or electron spin echo envelope modulation (ESEEM) measurements. There is of course no *a priori* reason why a_y should equal a_z or a_x, as the anisotropic contribution is expected to be different in each direction. However, our simulations did not give as good a fit for $a_x \neq a_y$, despite expectation.

The isotropic interaction, *via* the s orbitals, is given by equation (A6) where f_s is the fraction of the total spin density in

$$a_0 = (8\pi/3) f_s g_e g_n \beta_e \beta_n |\psi_s(0)|^2 \quad \text{(A6)}$$

the appropriate s orbital and $|\psi_s(0)|^2$ is the s-electron density at the ligand nucleus given 100% occupancy of the appropriate ligand s orbital. Values of $|\psi_s(0)|^2$ have been tabulated by *e.g.* Goodman and Raynor,[50] and the values of f_s can thus be calculated. The value of a_0 may be determined directly from the solution-phase spectra or, provided that the correct signs are used, from the components of the superhyperfine interaction as determined from the frozen-solution spectra. Values of f_s are given in Table 3.

The dipolar interaction is given by equation (A7) where R is

$$a_d = g_e \beta_e g_n \beta_n / R^3 \quad \text{(A7)}$$

the internuclear distance. We assume that the Tc–P distance in $[TcNCl_3(PPh_3)]$ is the same as the Re–P distance in $[ReNCl_2(PPh_3)_2]$, *viz.* 2.448 Å, and obtain $a_d = 0.73 \times 10^{-4}$ cm^{-1}. Also that the Tc–As distance in $[TcNCl_3(AsPh_3)]$ is the same as that in $[TcNCl_2(AsPh_3)_2]$, *viz.* 2.544 Å, which gives $a_d = 0.45 \times 10^{-4}$ cm^{-1}.

The values of $a_\sigma - a_\pi$ can thus be calculated, given the values of a_z and a_x determined by experiment. For P, $a_\sigma - a_\pi = -1.15 \times 10^{-4}$ cm^{-1}, whilst for As, $a_\sigma - a_\pi = -0.95 \times 10^{-4}$ cm^{-1}. The contributions from the σ and π orbitals cannot be separated experimentally. However, analogy with other systems suggests that $|a_\sigma| \ll |a_\pi|$.[33,48] The fractional density, f_p, on a p orbital is given by equation (A8) where a_p is the measured superhyperfine constant and $\langle r^{-3} \rangle$ is the expectation value for the appropriate p orbital. Values of $\langle r^{-3} \rangle$ are given by Goodman and Raynor[50] and values of f_p are given in Table 3.

$$a_p = \tfrac{4}{5} f_p g_e g_n \beta_e \beta_n \langle r^{-3} \rangle \quad \text{(A8)}$$

References

1 J. Baldas, J. F. Boas, J. Bonnyman and G. A. Williams, *J. Chem. Soc., Dalton Trans.*, 1984, 2395.
2 J. Baldas, J. Bonnyman and G. A. Williams, *Inorg. Chem.*, 1986, **25**, 150.
3 U. Abram, S. Abram, H. Spies, R. Kirmse, J. Stach and K. Köhler, *Z. Anorg. Allg. Chem.*, 1987, **544**, 167.
4 C. M. Archer, J. R. Dilworth, J. D. Kelly and M. McPartlin, *J. Chem. Soc., Chem. Commun.*, 1989, 375.
5 J. Baldas, S. F. Colmanet and M. F. Mackay, *J. Chem. Soc., Dalton Trans.*, 1988, 1725.
6 H.-J. Pietzsch, U. Abram, R. Kirmse and K. Köhler, *Z. Chem.*, 1987, **27**, 265.
7 J. Baldas, J. F. Boas, J. Bonnyman, S. F. Colmanet and G. A. Williams, *J. Chem. Soc., Chem. Commun.*, 1990, 1163.
8 R. Kirmse, J. Stach and U. Abram, *Polyhedron*, 1985, **4**, 1403.
9 U. Abram, R. Münze, R. Kirmse, K. Köhler, W. Dietzsch and L. Golič, *Inorg. Chim. Acta*, 1990, **169**, 49.
10 U. Abram, B. Lorenz, L. Kaden and D. Scheller, *Polyhedron*, 1988, **7**, 285.
11 D. T. Cromer and D. Liberman, *J. Chem. Phys.*, 1970, **53**, 1891.
12 R. J. Doedens and J. A. Ibers, *Inorg. Chem.*, 1967, **6**, 204.
13 G. M. Sheldrick, SHELX 76, Program for Crystal Structure Determination, University of Cambridge, 1976.
14 D. T. Cromer and J. B. Mann, *Acta Crystallogr., Sect. A*, 1968, **24**, 321.
15 *International Tables for X-Ray Crystallography*, Kynoch Press, Birmingham, 1974, vol. 4, p. 100.
16 R. F. Stewart, E. R. Davidson and W. T. Simpson, *J. Chem. Phys.*, 1965, **42**, 3175.
17 C. K. Johnson, ORTEP II, Fortran thermal-ellipsoid plot program, Oak Ridge National Laboratory, TN, 1976.
18 J. Baldas, J. F. Boas and J. Bonnyman, *J. Chem. Soc., Dalton Trans.*, 1987, 1721.
19 R. W. Thomas, M. J. Heeg, R. C. Elder and E. Deutsch, *Inorg. Chem.*, 1985, **24**, 1472.
20 P. M. Boorman, C. D. Garner and F. E. Mabbs, *J. Chem. Soc., Dalton*

Trans., 1975, 1299; C.-S. Kim and R. K. Murmann, *Inorg. Chem.*, 1984, **23**, 263.
21 J. Baldas, J. F. Boas and J. Bonnyman, *Aust. J. Chem.*, 1989, **42**, 639.
22 R. Kirmse, K. Köhler, R. Böttcher, R. Münze, U. Abram, M. C. M. Gribnau and K. P. Keijzers, in *Technetium and Rhenium in Chemistry and Nuclear Medicine 3*, eds. M. Nicolini, G. Bandoli and U. Mazzi, Cortina International, Verona, Raven Press, New York, 1990, p. 305.
23 U. Abram, R. Kirmse, K. Köhler, B. Lorenz and L. Kaden, *Inorg. Chim. Acta*, 1987, **129**, 15.
24 J. Baldas and S. F. Colmanet, *Aust. J. Chem.*, 1989, **42**, 1155.
25 G. A. Williams and J. Baldas, *Aust. J. Chem.*, 1989, **42**, 875.
26 J. Baldas, J. Bonnyman, M. F. Mackay and G. A. Williams, *Aust. J. Chem.*, 1984, **37**, 751.
27 U. Abram and R. Kirmse, *J. Radioanal. Nucl. Chem., Articles*, 1988, **122**, 311.
28 R. Kirmse, J. Stach and U. Abram, *Inorg. Chim. Acta*, 1986, **117**, 117.
29 J. Baldas, J. F. Boas, S. F. Colmanet and M. F. Mackay, *Inorg. Chim. Acta*, 1990, **170**, 233.
30 M. I. Scullane, R. D. Taylor, M. Minelli, J. T. Spence, K. Yamanouchi, J. H. Enemark and N. D. Chasteen, *Inorg. Chem.*, 1979, **18**, 3213.
31 D. Collison, F. E. Mabbs, J. H. Enemark and W. E. Cleland, jun., *Polyhedron*, 1986, **5**, 423.
32 K. Dehnicke, H. Prinz, W. Kafitz and R. Kujanek, *Liebigs Ann. Chem.*, 1981, 20.
33 J. R. Shock and M. T. Rogers, *J. Chem. Phys.*, 1973, **58**, 3356.
34 J. Zah-Letho, E. Samuel and J. Livage, *Inorg. Chem.*, 1988, **27**, 2233.
35 E. Samuel, G. Labauze and J. Livage, *Nouv. J. Chim.*, 1977, **1**, 93.
36 G. Labauze, E. Samuel and J. Livage, *Inorg. Chem.*, 1980, **19**, 1384.
37 M. A. Hitchman, C. D. Olson and R. L. Belford, *J. Chem. Phys.*, 1969, **50**, 1195.
38 D. Kivelson and S.-K. Lee, *J. Chem. Phys.*, 1964, **41**, 1896.
39 S. F. Colmanet and G. A. Williams, in *Technetium and Rhenium in Chemistry and Nuclear Medicine 3*, eds. M. Nicolini, G. Bandoli and U. Mazzi, Cortina International, Verona, Raven Press, New York, 1990, p. 55.
40 M. Melnik and J. E. Van Lier, *Coord. Chem. Rev.*, 1987, 77 275.
41 A. S. Batsanov, Yu. T. Struchkov, B. Lorenz and B. Olk, *Z. Anorg. Allg. Chem.*, 1988, **564**, 129.
42 E. Forsellini, U. Casellato, R. Graziani and L. Magon, *Acta Crystallogr., Sect. B*, 1982, **38**, 3081.
43 P. W. R. Corfield, R. J. Doedens and J. A. Ibers, *Inorg. Chem.*, 1967, **6**, 197.
44 R. C. Elder, R. Whittle, K. A. Glavan, J. F. Johnson and E. Deutsch, *Acta Crystallogr., Sect. B*, 1980, **36**, 1662.
45 K. A. Glavan, R. Whittle, J. F. Johnson, R. C. Elder and E. Deutsch, *J. Am. Chem. Soc.*, 1980, **102**, 2103.
46 C. M. Archer, J. R. Dilworth, J. D. Kelly and M. McPartlin, *Polyhedron*, 1989, **8**, 1879.
47 B. R. McGarvey, *J. Phys. Chem.*, 1967, **71**, 51.
48 P. T. Manoharan and M. T. Rogers, *J. Chem. Phys.*, 1968, **49**, 5510.
49 T. P. P. Hall, W. Hayes, R. W. H. Stevenson and J. Wilkens, *J. Chem. Phys.*, 1963, **38**, 1977.
50 B. A. Goodman and J. B. Raynor, *Adv. Inorg. Chem. Radiochem.*, 1970, **13**, 135.

Received 18*th March* 1991; *Paper* 1/01293B